Smart Mater. Struct. 17 (2008) 065016 (14pp) doi:10.1088/0964-1726/17/6/065016

Issues in mathematical modeling of piezoelectric energy harvesters

A Erturk[1,3] **and D J Inman**[2]

[1] Department of Engineering Science and Mechanics, Center for Intelligent Material Systems and Structures, Virginia Tech, Blacksburg, VA 24061, USA
[2] Department of Mechanical Engineering, Center for Intelligent Material Systems and Structures, Virginia Tech, Blacksburg, VA 24061, USA

E-mail: erturk@vt.edu

Received 28 May 2008, in final form 13 August 2008
Published 22 October 2008
Online at stacks.iop.org/SMS/17/065016

Abstract
The idea of vibration-to-electric energy conversion for powering small electronic components by using the ambient vibration energy has been investigated by researchers from different disciplines in the last decade. Among the possible transduction mechanisms, piezoelectric transduction has received the most attention for converting ambient vibrations to useful electrical energy. In the last five years, there have been a considerable number of publications using various models for the electromechanical behavior of piezoelectric energy harvester beams. The models used in the literature range from elementary single-degree-of-freedom (SDOF) models to approximate distributed parameter models as well as analytical distributed parameter solution attempts. Because of the diverse nature of researchers working in energy harvesting (including electrical, mechanical and materials engineers), several oversimplified and incorrect physical assumptions have been propagated in the literature. Issues of the correct formulation for piezoelectric coupling, correct physical modeling, use of low fidelity models, incorrect base motion modeling, and the use of static expressions in a fundamentally dynamic problem are discussed and clarified here. These common indiscretions, which have been repeated in the existing piezoelectric energy harvesting literature, are addressed and clarified with improved models, and examples are provided. This paper aims to provide corrections and necessary clarifications for researchers from different engineering disciplines interested in electromechanical modeling of piezoelectric energy harvesters.

(Some figures in this article are in colour only in the electronic version)

1. Introduction

Recent developments in power electronics have reduced the power requirements of small electronic components (such as the wireless sensors used in structural health monitoring) and motivated the research on powering these devices by using the vibration energy available in their environment. The ultimate goal is to remove the external power source or battery replacement requirement for such small electronic devices, especially in remote locations. The basic transduction mechanisms that can be used to convert the ambient vibration energy to electrical energy are electromagnetic, electrostatic and piezoelectric transductions. Among these transduction mechanisms, piezoelectric transduction has received the greatest attention in the last five years, and review articles summarizing the relevant work on piezoelectric energy harvesting can be found in the literature (see, for instance, Anton and Sodano [1]).

The research community working on piezoelectric energy harvesting is a very rapidly growing community, and it includes researchers from mechanical, electrical, materials and civil engineering areas. Other than the applications of piezoelectric energy harvesting, several researchers from different disciplines have studied modeling of piezoelectric energy harvesters. Certain issues have been observed in some of the existing models, and moreover, it has been noted that some very misleading models have been repeated by different researchers. The motivation here is therefore to discuss the

[3] Author to whom any correspondence should be addressed.

modeling problems and provide the necessary corrections for the research community interested in analytical modeling of piezoelectric energy harvesters.

In the following sections, the existing problems are investigated under two topics as *issues in SDOF modeling* and *issues in distributed parameter modeling*. The relevant concerns are addressed and clarifications are provided, with improved models and demonstrations. SDOF modeling problems include the incorrect representation of piezoelectric coupling and deficiencies originating from the well-known SDOF base excitation relation. As an alternative to the relatively low fidelity SDOF models, single-mode relations obtained from the distributed parameter solution are presented. The section related to SDOF modeling is given as a prelude to the more important discussion dealing with distributed parameter modeling.

Although SDOF modeling provides useful insight into the harvesting problem, it is required to derive a distributed parameter model to predict and investigate the electromechanical behavior of piezoelectric energy harvesters accurately. Consequently, several researchers have studied developing a distributed parameter model based on Euler–Bernoulli beam theory and the constitutive laws of piezoelectricity. The distributed parameter modeling approaches published include analytical solution attempts as well as approximate solutions in the sense of Rayleigh–Ritz discretization. The issues in distributed parameter modeling include avoiding the use of modal expansion and the resonance phenomenon, not modeling the piezoelectric coupling in the mechanical equation or oversimplifying the coupling as viscous damping, modeling of the mechanical forcing term due to base excitation as a tip force, use of static sensing and actuation equations, and the use of a static deflection pattern for a dynamics problem. Some of the above problems have caused fundamentally incorrect conclusions in the published literature. For instance, omitting the resonance phenomenon yields a totally different power frequency response function and therefore faulty conclusions. As another example, if the effect of piezoelectric coupling is not modeled in the mechanical (beam) equation, the variation of the resonance frequency with load resistance cannot be predicted. One particular phenomenon not predicted by low fidelity models is the amplification of the motion amplitude at the open circuit resonance frequency with increasing load resistance. The only way of predicting this phenomenon requires accurate consideration of piezoelectric coupling in the mechanical domain. In addition, the optimum resistive load that gives the maximum power is inaccurately predicted if the piezoelectric coupling in the beam equation is not modeled or oversimplified as a viscous damping term. These issues and others are discussed and clarified with improved models and examples in the following.

2. Issues in SDOF modeling

Since the electrical domain of the coupled piezoelectric energy harvesting problem consists of lumped parameters (internal capacitance of the piezoceramic and an external load resistance), representing the mechanical domain with lumped parameters (as a mass–spring–damper system) has been a useful modeling approach to obtain a fundamental understanding of the system dynamics. Issues in SDOF modeling include, but are not limited to, the use of electromagnetic generator equations to represent piezoelectric systems and different sources of inaccuracies due to the mechanical representation of the base excitation problem for cantilevered structures. This section clarifies the faults in using these assumptions.

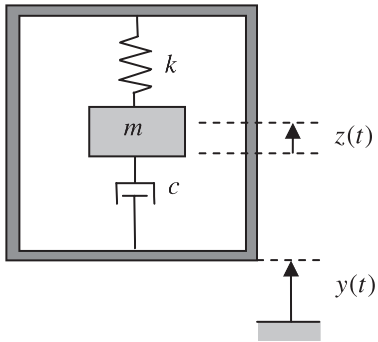

Figure 1. Schematic of an electromagnetic generator proposed by Williams and Yates [2].

2.1. An SDOF electromagnetic generator model

In their early work on the subject, Williams and Yates [2] briefly described the three possible transduction mechanisms that can be used for vibration-to-electric energy conversion as electromagnetic, electrostatic and piezoelectric transductions. They [2] 'chose to use the *electromagnetic* type of transduction' and presented a simple electromagnetic generator model. In their analysis, Williams and Yates [2] considered a magnetic seismic mass moving inside a coil as the micro-electric generator (figure 1). They used the well-known SDOF base excitation relation for describing the motion of the seismic mass with respect to the generator housing as

$$m\ddot{z} + c\dot{z} + kz = -m\ddot{y} \tag{1}$$

where m is the seismic mass, k is the spring constant, c is the viscous damping coefficient, y is the displacement of the vibrating generator housing, z is the displacement of the seismic mass relative to the generator housing, and a dot above a variable represents differentiation with respect to time. The combined effect of electrical and mechanical damping is considered in the damping coefficient c. This is a fairly accurate model for the electromagnetic generator type (magnet–coil configuration) analyzed by Williams and Yates [2]. A reasonable assumption in electromagnetic energy harvesting from a magnet–coil system is that the backward coupling in the mechanical domain is proportional to velocity *only*. Hence the electrical effect due to the presence of a resistive load can be represented by an electrically induced viscous damping coefficient in the mechanical equation of motion[4]. This convenient assumption makes it possible to express the magnet displacement frequency response function (FRF) per base acceleration and the average power FRF converted from the mechanical domain to the electrical domain as

$$\left|\frac{z}{\ddot{y}}\right| = \left|\frac{z}{-\omega^2 Y_0}\right| = \frac{1/\omega_n^2}{\sqrt{\left[1-(\omega/\omega_n)^2\right]^2 + \left[2\zeta\,(\omega/\omega_n)\right]^2}} \quad (2)$$

$$\left|\frac{P_{ave}}{\ddot{y}^2}\right| = \left|\frac{c_e \dot{z}^2/2}{\omega^4 Y_0^2}\right| = \frac{m\zeta_e \omega^2/\omega_n^3}{\left[1-(\omega/\omega_n)^2\right]^2 + \left[2\zeta\,(\omega/\omega_n)\right]^2} \quad (3)$$

where Y_0 is the amplitude of harmonic base displacement at frequency ω and c_e is the electrically induced damping coefficient such that the total damping coefficient in equation (1) can be separated as $c = c_m + c_e$, where c_m is the mechanical part of the damping coefficient c in equation (1). Note that, in equations (2) and (3), $\zeta = c/2\sqrt{km}$ is the total damping ratio, $\zeta_e = c_e/2\sqrt{km}$ is the damping ratio due to electromagnetic transduction, and ω_n is the undamped natural frequency due to $\omega_n = \sqrt{k/m}$. It is clear from equation (2) that the backward coupling information in the mechanical FRF is simply embedded in the viscous damping term ζ since $\zeta = \zeta_e + \zeta_m$.

The foregoing simple generator model is suitable for electromagnetic energy harvesting in which a magnetic seismic mass moves inside a coil due to the vibratory motion of the generator housing. The Williams and Yates model [2] has led to extended discussions on the power output and the effect of mechanical damping in the vibration energy harvesting literature [3]. However, the foregoing model and the relevant discussion in the literature are restricted to *electromagnetic generators* of the aforementioned type. Unfortunately, several researchers have wrongly used the electromagnetic model in their work on piezoelectric energy generation, which is an entirely different physical phenomenon.

2.2. Use of the SDOF electromagnetic generator model for piezoelectric energy harvesting

Piezoelectric transduction uses different physics than *electromagnetic* transduction. The mechanism of piezoelectric transduction is due to the constitutive relations [4] emerging from the material itself. As will be presented, the backward coupling effect of piezoelectric energy harvesting in the mechanical domain is not necessarily proportional to velocity only (i.e., it cannot be represented by just an electrically induced viscous damper). However, the SDOF electromagnetic generator model proposed by Williams and Yates [2] has been used in some papers on piezoelectric energy harvesting. In a recent work, Jeon *et al* [5] presented their micro-scale piezoelectric energy harvester that uses interdigitated electrodes to utilize the more effective 33-mode in bending. Later, Fang *et al* [6] introduced their micro-scale unimorph harvester which is operated in classical bending mode (31-mode). In both studies, the authors used the electromagnetic generator equations

[4] The form of equation (1) has other assumptions from the mechanical side of the problem (e.g., it assumes the spring to be massless and the seismic mass to undergo small oscillations so that the stiffness of the spring is constant).

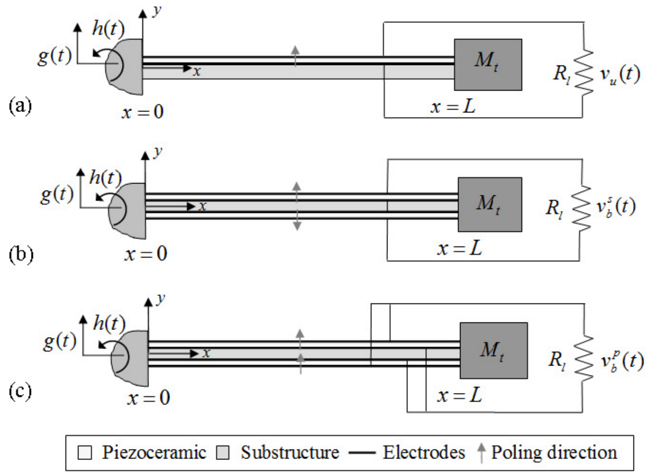

Figure 2. Cantilever piezoelectric energy harvester configurations under base excitation: (a) unimorph, (b) bimorph (series connection) and (c) bimorph (parallel connection) [8, 9].

of Williams and Yates [2] along with figure 1 to represent a simple mathematical model for piezoelectric energy harvesting. More recently, in a review article on piezoelectric energy harvesting, Priya [7] described figure 1 as 'the schematic of the piezoelectric generator' and discussed the Williams and Yates model as a 'generalized' model for conversion of vibration energy into electrical energy although the authors [2] did not have such a claim in the original work.

The reason we stress the incorrect use of equation (1) is to prevent future researchers from using this expression to model piezoelectric-based energy harvesters and hence from obtaining false theoretical results. The effect of electrical energy generation can be represented by a viscous damper in the mechanical domain *only* for magnet–coil type electromagnetic harvester configurations. Therefore, equation (1) does not describe a *generalized* model for vibration-to-electric energy conversion.

2.3. On the mechanism of piezoelectric transduction

The effect of piezoelectric coupling in the mechanical equation of motion is more sophisticated than that of electromagnetic coupling. Figure 2 shows the basic piezoelectric energy harvester configurations (unimorph and bimorph) under base excitation. The base excitation is due to the motion of the host structure (on which the harvester is attached) and it is represented in figure 2 in the form of translation in the transverse direction with small rotation as studied by Erturk and Inman [8, 9]. Typically, in most of the literature, only the translational component has been considered by assuming no base rotation. The conductive electrodes covering the top and the bottom faces of the piezoceramic layer(s) are connected to a resistive electrical load. Note that, depending on the poling direction of the piezoceramic layers and combination of the electrode leads, the piezoceramic layers of the bimorph configuration can be combined either in series or in parallel.

Basically, such a cantilevered harvester (a unimorph or a bimorph) is located on a vibrating host structure, and the dynamic strain induced in the piezoceramic layer(s) due to base excitation results in an alternating voltage output. The source of coupling in piezoelectric energy harvesting is the constitutive relations of the piezoceramic material. Based on Euler–Bernoulli beam assumptions (i.e., the classical thin beam model), the tensorial representation of the constitutive relations [4] can be reduced to the following two scalar equations for harvester beams operating in 31-mode (e.g., figure 2)

$$\begin{Bmatrix} T_1 \\ D_3 \end{Bmatrix} = \begin{bmatrix} c_{11}^{E} & -e_{31} \\ e_{31} & \varepsilon_{33}^{S} \end{bmatrix} \begin{Bmatrix} S_1 \\ E_3 \end{Bmatrix} \tag{4}$$

where T_1 is the stress component, D_3 is the electric displacement component, S_1 is the strain component, E_3 is the electric field component, e_{31} is the piezoelectric constant, c_{11}^{E} is the elastic stiffness component (Young's modulus) at constant electric field, and ε_{33}^{S} is the permittivity component at constant strain. Furthermore, the directions 1 and 3 coincide with the longitudinal (x) and the transverse (y) directions of the beam in figure 2, respectively. According to equation (4), a mechanical strain field induced in the piezoceramic layer results in an electric displacement field throughout its length. Meanwhile, an electric field develops across the conductive electrodes in the thickness direction and it sends feedback to the mechanical domain and affects the mechanical stress field. In the light of equation (4), one can anticipate that the effect of piezoelectric coupling in the mechanical domain does not have to be in the form of viscous damping. Indeed, developing a distributed parameter model by integrating the electric displacement in equation (4) over the electrode area and the moment of mechanical stress over the beam cross-section makes it possible to observe the distinctions of the effects of piezoelectric coupling on beam vibrations [8, 9]. One important distinction is due to the short circuit and the open circuit resonance frequencies. As the load resistance in the electrical circuit is increased from zero to infinity, reasonably, the system moves from short circuit to open circuit conditions. This is associated with a *variation* in the modal frequencies (of the harvester beam) from the short circuit to the open circuit resonance frequencies. Although increasing the load resistance attenuates the motion amplitude at the short circuit resonance frequency up to a certain point, interestingly, it amplifies the motion amplitude at the open circuit resonance frequency [8, 9] (see section 3.2). Load–resistance dependent variation of the resonance frequencies and amplification of the motion at the open circuit resonance frequency with increasing load resistance are strong indicators of the fact that the effect of piezoelectric coupling in the mechanical domain is more complicated than simple viscous damping.

2.4. An improved SDOF piezoelectric energy harvester model

An SDOF piezoelectric energy harvester model was introduced by duToit *et al* [10], in which they considered the mechanism of piezoelectric coupling in a simple way. Figure 3 shows the schematic of their cantilevered harvester, which is excited by the motion of its base in the longitudinal direction. Therefore, rather than bending, this model uses *longitudinal* vibrations of a piezoceramic (like a typical accelerometer). As the direction

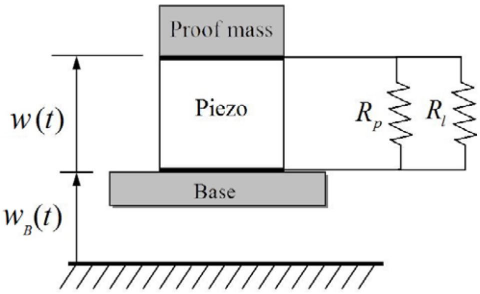

Figure 3. Schematic of the 1D harvester model proposed by duToit *et al* [10].

of mechanical strain and the electric field are coincident, the harvester model shown in figure 3 uses the 33-mode (and therefore the d_{33} constant of the piezoceramic) where the 3-direction is the longitudinal direction. The electrodes are connected to an equivalent resistive load R_{eq} (which is the parallel combination of piezoceramic leakage resistance R_{p} and load resistance R_{l}, where $R_{\mathrm{l}} \ll R_{\mathrm{p}}$; hence $R_{\mathrm{eq}} \approx R_{\mathrm{l}}$). The coupled SDOF equations are given by duToit *et al* [10] as

$$\ddot{w} + 2\zeta_{\mathrm{m}}\omega_{\mathrm{n}}\dot{w} + \omega_{\mathrm{n}}^2 w - \omega_{\mathrm{n}}^2 d_{33} v = -\ddot{w}_{\mathrm{B}} \tag{5}$$

$$R_{\mathrm{eq}} C_{\mathrm{p}} \dot{v} + v + m_{\mathrm{eff}} R_{\mathrm{eq}} d_{33} \omega_{\mathrm{n}}^2 \dot{w} = 0 \tag{6}$$

where w_{B} is the base displacement, w is the displacement of the proof mass relative to the base, v is the voltage output, m_{eff} is the effective mass, ζ_{m} is the mechanical damping ratio, ω_{n} is the undamped natural frequency, and C_{p} is the capacitance of the piezoceramic. Comparing equations (1) and (5) shows that equation (5) still relies on the SDOF base excitation relation. However, the backward coupling effect of the voltage generated is considered in equation (5) in a convenient manner with the additional term $\omega_{\mathrm{n}}^2 d_{33} v$. For a harmonic base displacement w_{B} at frequency ω, equations (5) and (6) give the coupled mechanical response FRF of the proof mass and the electrical power output FRFs (per harmonic base acceleration) as

$$\left|\frac{w}{\ddot{w}_{\mathrm{B}}}\right| = \frac{1/\omega_{\mathrm{n}}^2\sqrt{1+(r\Omega)^2}}{\sqrt{\left[1-(1+2\zeta_{\mathrm{m}}r)\,\Omega^2\right]^2 + \left[\left(1+k_{\mathrm{e}}^2\right)r\Omega + 2\zeta_{\mathrm{m}}\Omega - r\Omega^3\right]^2}} \tag{7}$$

$$\left|\frac{P}{(\ddot{w}_{\mathrm{B}})^2}\right| = \frac{m_{\mathrm{eff}} 1/\omega_{\mathrm{n}} r k_{\mathrm{e}}^2 R_{\mathrm{eq}}/R_{\mathrm{l}}\Omega^2}{\left[1-(1+2\zeta_{\mathrm{m}}r)\,\Omega^2\right]^2 + \left[\left(1+k_{\mathrm{e}}^2\right)r\Omega + 2\zeta_{\mathrm{m}}\Omega - r\Omega^3\right]^2} \tag{8}$$

where $\Omega = \omega/\omega_{\mathrm{n}}$ is the dimensionless frequency, k_{e} is the coupling coefficient, and $r = \omega_{\mathrm{n}} R_{\mathrm{eq}} C_{\mathrm{p}}$ [10]. Comparing equations (2) and (7) shows that the backward piezoelectric coupling acts in a more complicated way than viscous damping. Moreover, the denominator of equation (8) shows that the resonance of the power FRF for a given R_{l} *cannot*

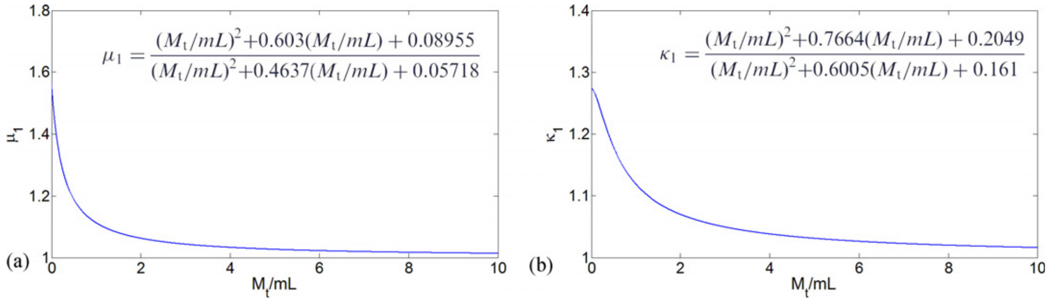

Figure 4. Variation of correction factors with proof mass to beam/bar mass ratio for (a) transverse and (b) longitudinal vibrations [11].

be predicted accurately if equation (3) is used. That is, for a given R_l, the maximum power is not necessarily obtained for $\omega = \omega_n$ (or not for $\omega = \omega_n\sqrt{1-\zeta_m^2}$) as the resonance frequency may change considerably with R_l. Using the above two simple equations, duToit *et al* [10] were able to observe the short circuit and open circuit resonance trends later observed by Erturk and Inman [8, 9] based on the analytical distributed parameter solution. As addressed in section 2.5, the well-known SDOF base excitation relation of the form given by equation (5) (or equation (1)) fails to predict the forcing amplitude accurately if the tip mass (proof mass) to distributed mass ratio is not very high. Correction factors [11] were derived to improve the predictions of the above SDOF piezoelectric energy harvester model proposed by duToit *et al* [10].

Another improved SDOF cantilever model was presented by Roundy *et al* [12, 13] for a bimorph cantilever configuration (figures 2(b) and (c)) in transverse (bending) vibrations due to base excitation. In modeling, Roundy *et al* [13] did not model the distributed mass of the cantilever which *implicitly* assumes the tip mass (M_t in figure 2) to be much larger than the distributed mass of the cantilevered beam. Note that an inaccurate estimation of the harvester total mass may cause not only inaccurate estimation of the harvester's natural frequency, but may also result in inaccurate estimation of the excitation amplitude, since the forcing term in the base excitation problem is due to the mass of the harvester. Even though this model [13] was an introductory modeling attempt for harvesters operating in bending mode, just like the model proposed by duToit *et al* [10], it also showed that the electrical power expression for piezoelectric energy harvesting is not as simple as equation (3).

2.5. Further issues in SDOF modeling

The problems regarding SDOF modeling are not limited to the representation of piezoelectric coupling. One particular issue is due to the deficiency of using the well-known SDOF base excitation relation. The governing equation for the base excitation problem of a mass–spring–damper system (figure 1) is given by equation (1). In the presence of piezoelectric coupling, duToit *et al* [10] modified this expression to equation (5) by adding the relevant voltage term. Yet, the origin of equation (5) is clearly equation (1), which is the SDOF base excitation relation. Based on distributed parameter modeling of the uncoupled mechanical problem, Erturk and Inman [11] recently showed that, if the proof mass of the harvester is not much larger than the mass of a cantilevered beam in transverse vibrations (or a cantilevered bar in longitudinal vibrations), the form of equation (1) yields highly inaccurate results. The inaccuracy is due to the contribution of the spring mass (i.e., the distributed beam/bar mass) to the excitation amplitude, which becomes very important if the proof mass is not very large. It was proposed [11] that the SDOF *uncoupled* governing equation (which is equation (1) in this paper) should be modified such that, for a uniform cantilevered beam in transverse vibrations,

$$m\ddot{z} + c\dot{z} + kz = -\mu_1 m\ddot{y} \tag{9}$$

and for a uniform cantilevered bar in longitudinal vibrations,

$$m\ddot{z} + c\dot{z} + kz = -\kappa_1 m\ddot{y} \tag{10}$$

where μ_1 and κ_1 are the correction factors (for transverse and longitudinal vibrations, respectively). These factors correct the excitation amplitude with a mode shape dependent consideration of the distributed mass, and subscript 1 is for the mode number (the fundamental mode here). Note that, in the absence of a proof mass, $\mu_1 = 1.566$ and $\kappa_1 = 1.273$. Hence, even if the natural frequency prediction was correct[5], in the absence of a proof mass, the tip motion would be underestimated with an error of 36% for transverse vibrations and with an error of 21% for longitudinal vibrations [11]. As depicted in figure 4 (along with curve fit relations), the correction factors depend on the proof mass to beam/bar mass ratio, and they tend to unity as this ratio becomes very large. That is, there is no need to correct the excitation amplitude if the harvester beam/bar has a large proof mass. Reasonably, if the proof mass is very large, its inertia (as the source of excitation due to base motion) dominates the total inertia of the cantilevered harvester, and the distributed inertia of the beam/bar becomes negligible.

The SDOF correction factor κ_1 is then applied to the excitation amplitude of the coupled mechanical equation given

[5] In the absence of a proof mass, Rayleigh's [14] effective mass relation for the transverse vibrations case (i.e., 33/140 of the beam mass) results in an acceptable error of 0.5% in the natural frequency prediction (compared to the exact Euler–Bernoulli beam solution). However, the effective mass relation for the longitudinal vibrations (i.e., 1/3 of the bar mass) yields a fundamental natural frequency with an error of about 10.3% compared to the exact solution of the respective partial differential equation (in the absence of a proof mass).

by equation (5) as

$$\ddot{w} + 2\zeta_{\mathrm{m}}\omega_{\mathrm{n}}\dot{w} + \omega_{\mathrm{n}}^2 w - \omega_{\mathrm{n}}^2 d_{33} v = -\kappa_1 \ddot{w}_{\mathrm{B}}. \quad (11)$$

After this improvement, κ_1 and κ_1^2 appear in the numerators of equations (7) and (8), respectively. Otherwise, both the vibratory motion of the harvester and the resulting voltage and power outputs are underestimated. In their modeling work, duToit *et al* [10] presented a numerical case study for their harvester operating in the longitudinal mode (figure 3). In their case study [10], the proof mass to bar mass ratio was $M_{\mathrm{t}}/mL = 1.33$, which is not large enough to ignore the respective correction factor according to figure 4(b). It was shown [11] that the excitation amplitude in that particular case study should be corrected with a factor of $\kappa_1 = 1.0968$. Theoretically, this modification avoids underestimation of the tip motion and the voltage amplitudes with an error of 8.83% and the resulting power amplitude with an error of 16.9% [11].

As an additional point, the base excitation problem yields an excitation term that is due to external viscous damping [11]. Compared to the inertial excitation term, the damping related excitation is negligible for cantilevers operating in fluids with less damping effect, such as air. For a uniform cantilever without a tip mass, it was shown in a dimensionless basis that the contribution from air damping to the excitation at resonance is less than 5% of the total (inertial and damping) excitation if the damping ratio due to air damping is less than 2.5% (see figure 3 in [11]). The presence of a tip mass reduces the percentage contribution of this external damping related excitation term to the modal forcing function even more. Recently, duToit and Wardle [15] identified 1.78% total damping for a cantilevered bimorph, and Erturk and Inman [9] identified 2.7% total damping for a similar cantilevered bimorph with a tip mass (for the fundamental mode). Hence, one can conclude that the damping ratio due to air damping is typically less than these values and that the excitation due to air damping is negligible for harvesters operating in air. However, one should be careful when analyzing harvesters (under base excitation) operating in fluids with larger damping effect.

2.6. Single-mode equations based on the distributed parameter solution

Recently, the closed-form distributed parameter solutions (based on Euler–Bernoulli beam theory) have been obtained [8, 9] for the configurations shown in figure 2. The coupled steady state response expressions to harmonic excitation at an arbitrary frequency (given in section 3.6) are simplified for modal excitations (i.e., for excitations at or around the natural frequencies) to obtain *single-mode* relations. The single-mode relations proposed by Erturk and Inman [8, 9] are as accurate as the multi-mode solutions (section 3.6) for excitations in the vicinity of a modal (natural) frequency of interest [9]. For instance, for the unimorph cantilever shown in figure 2(a), the closed-form analytical solution for the coupled displacement response $\hat{w}_{\mathrm{rel}}(x,t)$ at an arbitrary point on the harvester beam (relative to the base) and the voltage response $\hat{v}_{\mathrm{u}}(t)$ across the resistive load are given by equations (12) and (13), respectively:

$$\hat{w}_{\mathrm{rel}}(x,t) = \frac{(1+\mathrm{j}\omega\tau_{\mathrm{c}})\, m\omega^2\gamma_{\mathrm{r}}^{w}\phi_{\mathrm{r}}(x)}{\mathrm{j}\omega\tau_{\mathrm{c}}\chi_{\mathrm{r}}\varphi_{\mathrm{r}} + (1+\mathrm{j}\omega\tau_{\mathrm{c}})\left(\omega_{\mathrm{r}}^2 - \omega^2 + \mathrm{j}2\zeta_{\mathrm{r}}\omega_{\mathrm{r}}\omega\right)} Y_0 \mathrm{e}^{\mathrm{j}\omega t} \quad (12)$$

$$\hat{v}_{\mathrm{u}}(t) = \frac{\mathrm{j}\tau_{\mathrm{c}} m\omega^3\varphi_{\mathrm{r}}\gamma_{\mathrm{r}}^{w}}{\mathrm{j}\omega\tau_{\mathrm{c}}\chi_{\mathrm{r}}\varphi_{\mathrm{r}} + (1+\mathrm{j}\omega\tau_{\mathrm{c}})\left(\omega_{\mathrm{r}}^2 - \omega^2 + \mathrm{j}2\zeta_{\mathrm{r}}\omega_{\mathrm{r}}\omega\right)} Y_0 \mathrm{e}^{\mathrm{j}\omega t} \quad (13)$$

where hat (^) denotes that the equations are *reduced* for modal excitations ($\omega \cong \omega_{\mathrm{r}}$), the subscript u is for unimorph (in agreement with figure 2(a)), r is the vibration mode of interest, and the relevant terms can be found in [8]. Note that the above expressions assume the base excitation to be in the form of harmonic translation $g(t) = Y_0 \mathrm{e}^{\mathrm{j}\omega t}$ with no rotation (i.e., $h(t) = 0$); however, small rotation of the base can be incorporated easily [8, 9]. From equations (12) and (13), the displacement and the electrical power FRFs (per harmonic base acceleration) can be obtained as

$$\left|\frac{\hat{W}_{\mathrm{rel}}(x)}{-\omega^2 Y_0}\right| = \left\{ m\left|\gamma_{\mathrm{r}}^{w}\phi_{\mathrm{r}}(x)\right|\sqrt{1+(\omega\tau_{\mathrm{c}})^2}\right\} \times \left\{\left[\omega_{\mathrm{r}}^2 - \omega^2\left(1+2\tau_{\mathrm{c}}\zeta_{\mathrm{r}}\omega_{\mathrm{r}}\right)\right]^2 + \left[2\zeta_{\mathrm{r}}\omega_{\mathrm{r}}\omega + \tau_{\mathrm{c}}\omega\left(\chi_{\mathrm{r}}\varphi_{\mathrm{r}} + \omega_{\mathrm{r}}^2 - \omega^2\right)\right]^2\right\}^{-1/2} \quad (14)$$

$$\left|\frac{\hat{P}}{\omega^4 Y_0^2}\right| = \left\{ C_{\mathrm{p}}\tau_{\mathrm{c}}\left(m\varphi_{\mathrm{r}}\gamma_{\mathrm{r}}^{w}\omega\right)^2\right\}\left\{\left[\omega_{\mathrm{r}}^2 - \omega^2\left(1+2\tau_{\mathrm{c}}\zeta_{\mathrm{r}}\omega_{\mathrm{r}}\right)\right]^2 + \left[2\zeta_{\mathrm{r}}\omega_{\mathrm{r}}\omega + \tau_{\mathrm{c}}\omega\left(\chi_{\mathrm{r}}\varphi_{\mathrm{r}} + \omega_{\mathrm{r}}^2 - \omega^2\right)\right]^2\right\}^{-1}. \quad (15)$$

It is worth stressing that the origin of the above single-mode expressions is the distributed parameter solution (not the SDOF base excitation modeling). This is the reason that the term 'single-mode' is used and these equations represent the multi-mode expressions given in section 3.6 accurately for the rth vibration mode [9]. The particular interest in energy harvesting is the fundamental vibration mode, which corresponds to the $r = 1$ case in equations (14) and (15). It is worth highlighting the qualitative similarity of the SDOF equations (7) and (8) derived by duToit *et al* [10] and the distributed parameter single-mode equations (14) and (15) derived by Erturk and Inman [8]. This is an indication of the fact that the simpler model proposed by duToit *et al* [10] was fairly successful in describing the piezoelectric coupling of the electromechanical system in the qualitative sense. However, the SDOF equations (7) and (8) lack the important information involved in the single-mode equations (14) and (15), such as the accurate strain distribution, mode shape and electrode location dependence of electromechanical coupling, besides the fact that the former equation pair was given for longitudinal vibrations.

3. Issues in distributed parameter modeling

Although SDOF modeling gives initial insight into the coupled problem, accurate electromechanical modeling of a

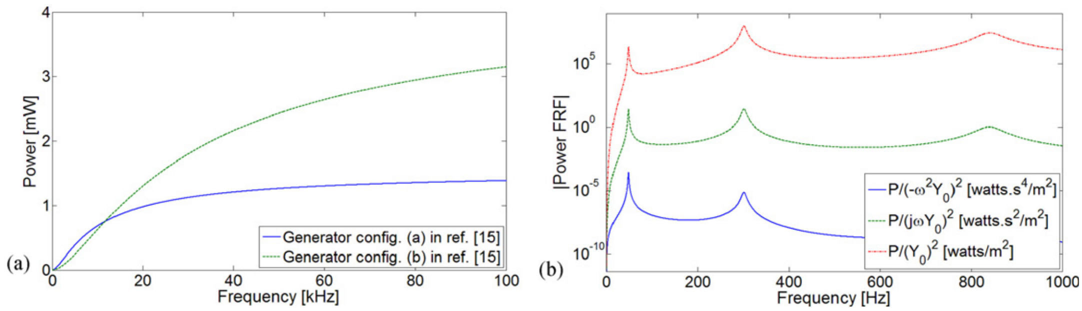

Figure 5. Sample power FRFs from the analytical relations presented in (a) Lu *et al* [16] and (b) Erturk and Inman [8] for different case studies.

piezoelectric energy harvester requires using a distributed parameter modeling approach. The existing distributed parameter modeling approaches range from Rayleigh–Ritz type of discretization to analytical modeling attempts, and the modeling issues are due to the effect of modal expansion and the resonance phenomenon, oversimplification of piezoelectric coupling in the mechanical equation of motion, representation of base excitation as a forcing term, use of the existing static actuation equations, and inaccuracies due to using static beam deflection equations in the dynamic problem. These problems are addressed in this section, and improved models are introduced for the reader's reference.

3.1. Effects of higher vibration modes and the resonance phenomenon

Based on the *expansion theorem* of operator theory, the instantaneous deflection pattern of an elastic curve (the neutral axis of one of the harvester beam configurations in figure 2) can be represented by an absolutely and uniformly convergent series of orthogonal eigenfunctions as

$$w_{\mathrm{rel}}(x,t) = \sum_{r=1}^{\infty} \phi_{\mathrm{r}}(x)\eta_{\mathrm{r}}(t) \tag{16}$$

where $w_{\mathrm{rel}}(x,t)$ is the elastic transverse displacement of the neutral axis at point x and time t relative to the base of the cantilever (figure 2), $\phi_{\mathrm{r}}(x)$ is the eigenfunction, and $\eta_{\mathrm{r}}(t)$ is the modal response of the rth vibration mode [8, 9]. If one is *strictly* interested in the response to modal excitation (at the rth natural frequency ω_{r}), representing $w_{\mathrm{rel}}(x,t)$ as follows is fairly acceptable:

$$w_{\mathrm{rel}}(x,t) \cong \phi_{\mathrm{r}}(x)\eta_{\mathrm{r}}(t). \tag{17}$$

Otherwise, for arbitrary excitation frequencies away from ω_{r}, equation (17) estimates the response inaccurately because it takes the rth mode shape as the only basis of the deflection pattern and ignores all the other orthogonal modes. The form of the mechanical response given by equation (17) was assumed by different authors for relating the voltage or electrical power of cantilevered piezoelectric energy harvesters to vibration mode shape [16, 17]. Among the other issues in Lu *et al* [16], the ultimate expression that relates the electrical power to tip vibration amplitude of the cantilever is highly deceptive as it lacks not only the information of higher vibration modes but also, more importantly, it misses the *resonance phenomenon* completely due to incorrect representation of the tip vibration amplitude. The resulting average power $\bar{P}$ expression is obtained by Lu *et al* [16] as

$$\bar{P} = \frac{\omega^2 b^2 h^2 e_{31}^2 \bar{A}^2}{4(1 + bL\varepsilon_{33}\omega R/\Delta)^2} R \tag{18}$$

where $\bar{A}$ is the amplitude of the bending slope difference at the boundaries of the piezoceramic layer. The resonance phenomenon is supposed to be exhibited by the vibration frequency response ($\bar{A}$ in the above equation), and consequently, by the voltage and power FRFs as well. Lu *et al* [16] used equation (18) to compare two cantilevered piezoelectric energy harvester configurations theoretically. For the numerical parameters and a certain value of $\bar{A}$ from [16], the power frequency response is obtained by using equation (18), as shown in figure 5(a). In [16], Lu *et al* presented a similar graph to compare the power outputs of two generator configurations for low and high frequency excitations (see figure 6 in [16]). The cantilevered harvesters [16] had a resonance frequency of about 2939 Hz but *no resonance* was observed (as in figure 5(a) here) within a frequency range of 0–1000 kHz because the resonance information was lost due to using a constant amplitude for $\bar{A}$. Just like a vibration response FRF, an electrical power FRF displays the resonance behavior at the resonance frequencies of the harvester. As an example, the electrical power FRF of the unimorph cantilever analyzed in [8] is shown in figure 5(b) (for a resistive load of 10 kΩ). For convenience, the electrical power output of a cantilevered harvester under base excitation can be given per base motion input (in terms of base acceleration, velocity or displacement). Since the cantilevered harvester investigated in [8] has three natural frequencies in the frequency range 0–1000 Hz, the power FRF experiences three resonances in this frequency range. Similar trends are expected from the cantilevers analyzed by Lu *et al* [16] with the correct treatment based on the fundamental vibration theory. Formal treatment of the vibration problem using equation (17) could capture the resonance at the frequency of the vibration mode of interest. However, in order to account for all the vibration modes in the power FRF as depicted in figure 5(b), one should use the expansion of the vibration modes as in equation (16).

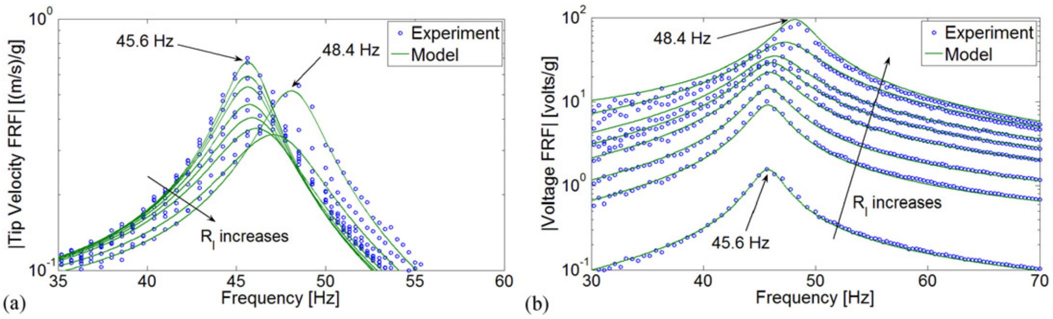

Figure 6. Variation of the (a) tip velocity FRF and the (b) voltage FRF with changing load resistance with a focus on the resonance frequency shift of a bimorph cantilever [9].

3.2. Oversimplification of piezoelectric coupling in the beam equation

The mechanism of piezoelectric coupling was discussed in section 2.3. One particular issue repeated in the literature is due to the lack of including piezoelectric coupling or its oversimplification as viscous damping in distributed parameter modeling [16–19]. For instance, in their distributed parameter modeling attempts based on Euler–Bernoulli beam theory, Lu *et al* [16], Lin *et al* [18] and Ajitsaria *et al* [19] did *not* consider the effect of *backward* piezoelectric coupling in the beam equation, which may result in very inaccurate predictions. Leaving out the piezoelectric coupling in the mechanical equation assumes the beam vibration to be totally unaffected by the electrical power generation process and violates the coupling coming from the piezoelectric constitutive laws (equation (4)). Chen *et al* [17] assumed the effect of piezoelectric coupling in the beam equation to be in the form of viscous damping, which is still an oversimplified assumption for distributed parameter modeling, as discussed in the following.

As mentioned in section 2.3, the piezoelectric constitutive relations do not necessarily imply a dissipative coupling effect that is proportional to velocity only. The complexity associated with piezoelectric coupling was observed in the denominators of the single-mode relations given by equations (14) and (15). Hence, it may yield inaccurate results to represent the effect of a resistive electrical load as a viscous damper in the mechanical equation. Figure 6(a) shows the tip velocity FRF (per base acceleration in gs) of a bimorph cantilever configuration (in the form of figure 2(b)) for different values of load resistance, as recently investigated by Erturk and Inman [9]. The variation of the voltage output FRF of the bimorph for the same set of resistive loads is presented in figure 6(b) [9]. These two figures focus on the fundamental vibration mode of the bimorph. Clearly, as the load resistance is increased (from 1 to 470 kΩ), the resonance frequency of the cantilever shifts from the short circuit resonance frequency (45.6 Hz) to the open circuit resonance frequency (48.4 Hz). Furthermore, it is very interesting to observe that, due to the shift in the resonance frequency, increasing load resistance amplifies the tip motion of the cantilever at the open circuit resonance frequency although it attenuates the motion up to a certain point for excitation at the short circuit resonance frequency. This resonance frequency shift *cannot* be captured by models which do not consider the backward piezoelectric coupling effect in the beam equation or oversimplify it as a viscous damping term. Since the resonance frequency for a given load resistance cannot be predicted accurately by oversimplifying the backward piezoelectric coupling effect [16–19], the frequency and amplitude of the maximum voltage and power (in the electrical FRF, such as the voltage FRF shown in figure 6(b)) are predicted inaccurately. As a result, such models [16–19] fail in estimating the maximum performance of a given piezoelectric energy harvester accurately. Note that the bimorph counterparts of the single-mode equations (14) and (15) (for series connection) were derived and used in [9] to predict the coupled system dynamics around the fundamental vibration mode as shown in figure 6. It is worth adding that the frequency shift mentioned here is a direct measure of the quality of the electromechanical coupling for a piezoelectric-based energy harvester.

Besides the deficiency in predicting the coupled system dynamics due to incorrect modeling (or viscous damping representation) of piezoelectric coupling [16–19], an important misinterpretation that originates from the same issue should be addressed briefly. Lu *et al* [16] and Lin *et al* [18] drew the same incorrect conclusion by not considering the backward piezoelectric coupling effect. They [16, 18] claimed that the optimum load resistance that gives the maximum power is $R_l^{opt} = 1/\omega C_p$, where ω is the excitation frequency and C_p is the internal capacitance of the piezoceramic layer. It is well known that a piezoelectric element can be represented as a current source in parallel with its internal capacitance or as a voltage source in series with its internal capacitance. However, one should be very careful with these representations in the electrical domain because the complete representation of the coupled electromechanical problem is actually a *transformer*. The current source term (in the respective representation) receives *feedback* from the voltage across the resistive load (connected to the electrodes), and the feedback sent to the mechanical domain depends on the load resistance, as depicted in figure 6(a). Ignoring the backward piezoelectric coupling and just adding a resistive load R_l to one of the aforementioned circuit representations results in an optimum load resistance of $R_l^{opt} = 1/\omega C_p$ for the maximum power, which is incorrect. One can easily demonstrate the inaccuracy of this expression. The optimum load resistance of the bimorph discussed with

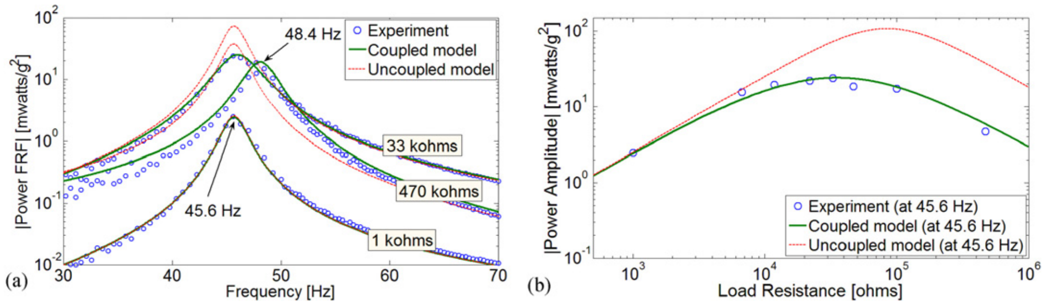

Figure 7. Comparison of the coupled and uncoupled distributed parameter model predictions for the bimorph used in [9]: (a) electrical power FRFs for three different resistive loads and (b) variation of the electrical power amplitude with load resistance for resonance excitation.

figures 6(a) and (b) was about 35 kΩ for excitation at 45.6 Hz (fundamental short circuit resonance frequency) and it was about 186 kΩ for excitation at 48.4 Hz (fundamental open circuit resonance frequency) as extracted experimentally and predicted successfully by the bimorph counterpart of equation (15) in [9]. However, the expression $R_1^{\mathrm{opt}} = 1/\omega C_\mathrm{p}$ presented in [16, 18] predicts the optimum values of load resistance for excitations at 45.6 and 48.4 Hz very inaccurately as 84.6 and 79.7 kΩ, respectively. Recently, this relation ($R_1^{\mathrm{opt}} = 1/\omega C_\mathrm{p}$) given by Lu *et al* [16] was referred to in a review article by Beeby *et al* [20] as the equation that shows how the optimum electrical load varies for different piezoelectric generators.

Figures 7(a) and (b) show the inaccuracy in the electrical power prediction by *not* considering the backward piezoelectric coupling effect in the distributed parameter beam equation. The model predictions and the experimental results given in figure 7 belong to the bimorph cantilever used in [9]. The electrical power FRFs for three different resistive loads are displayed in figure 7(a), where the uncoupled model is in agreement with the coupled one only for the lowest load resistance (1 kΩ). As the load resistance is increased, the electrical power prediction of the uncoupled model strongly deviates from that of the coupled model (and more importantly from the experimental results). Deviation of the uncoupled model as a function of load resistance is more clearly observed in figure 7(b) for excitation at the short circuit resonance frequency (45.6 Hz). As mentioned in the previous paragraph, the uncoupled model predicts the optimum load resistance for excitation at 45.6 Hz as 84.6 kΩ, which *overestimates* the optimum load resistance of the coupled system (35 kΩ) with an error of about 142%. Moreover, the uncoupled model overestimates the maximum power by more than a factor of 4. The distributed parameter model with backward coupling [9] is in very good agreement with the experimental results.

3.3. Representation of the mechanical forcing term due to base excitation

Since it is not one of the typical external loading types (such as a point force at the tip), the representation of base excitation as a forcing function has caused some confusion in the literature. As discussed by Erturk and Inman [8], in the absence of a tip mass, the forced partial differential equation of motion for the transverse displacement $w_{\mathrm{rel}}(x,t)$ of a uniform cantilevered beam relative to its base can be written as

$$YI\frac{\partial^4 w_{\mathrm{rel}}(x,t)}{\partial x^4} + c_\mathrm{s} I\frac{\partial^5 w_{\mathrm{rel}}(x,t)}{\partial x^4 \partial t} + c_a\frac{\partial w_{\mathrm{rel}}(x,t)}{\partial t} + m\frac{\partial^2 w_{\mathrm{rel}}(x,t)}{\partial t^2} + \vartheta v(t)\left[\frac{\mathrm{d}\delta(x)}{\mathrm{d}x} - \frac{\mathrm{d}\delta(x-L)}{\mathrm{d}x}\right] = -m\frac{\partial^2 w_b(x,t)}{\partial t^2} - c_a\frac{\partial w_b(x,t)}{\partial t} \tag{19}$$

where $w_b(x,t) = g(t) + xh(t)$ is the base displacement acting on the beam due to the translation $g(t)$ in the transverse direction with superimposed small rotation $h(t)$ (figure 2), and the remaining terms can be found in [8]. The right-hand-side forcing function is therefore a pressure distribution due to base excitation and it consists of an inertial term along with an external (air) damping related term. As discussed in section 2.5, the contribution from external damping to the forcing function is usually negligible (compared to the inertial term) for harvesters operating in air. Therefore, the effective force acting on the beam is basically a pressure distribution proportional to the mass distribution. The presence of a proof mass at the tip of the cantilever ($x = L$) creates a *jump* in the pressure distribution generated by the tip mass since m should be replaced by $m + M_\mathrm{t}\delta(x-L)$, where $\delta(x)$ is the Dirac delta function. In the presence of a tip mass, substituting equation (16) in (19) and applying the orthogonality conditions of the eigenfunctions $\phi_\mathrm{r}(x)$ yields an infinite set of ordinary differential equations for the modal response $\eta_\mathrm{r}(t)$:

$$\ddot{\eta}_\mathrm{r}(t) + 2\zeta_\mathrm{r}\omega_\mathrm{r}\dot{\eta}_\mathrm{r}(t) + \omega_\mathrm{r}^2\eta_\mathrm{r}(t) + \chi_\mathrm{r} v(t) = -\frac{\mathrm{d}^2 g(t)}{\mathrm{d}t^2}\left(m\int_0^L \phi_\mathrm{r}(x)\mathrm{d}x + M_\mathrm{t}\phi_\mathrm{r}(L)\right) \tag{20}$$

where the base rotation is assumed to be zero (i.e., $h(t) = 0$) and the forcing term due to air damping is neglected (the general form and the relevant terms can be found in [8]). This short discussion completes the analytical treatment of base excitation as a forcing term in distributed parameter modeling. Hence, the above treatment should be preferred to representing the base excitation as a tip force acting in the transverse direction. As an example from the literature, recently, Ajitsaria *et al* [19] multiplied the SDOF prediction of the tip acceleration and the effective tip mass to represent the base excitation rather than following the foregoing formal procedure. Indeed, when the component of the forcing term due to proof mass is much larger than the component due to the distributed mass, one can estimate the forcing function by considering the proof mass component only. However, it is important to note that the proof mass, as a point force at the tip, multiplies the base acceleration in equation (20), not the tip acceleration [19].

Other than the analytical distributed parameter modeling attempts mentioned here, the Rayleigh–Ritz type of discretization proposed by Hagood *et al* [21] (based on Hamilton's principle for electromechanical systems given by Crandall *et al* [22]) was employed for piezoelectric energy harvesting [10, 23, 24]. The first implementation of the Rayleigh–Ritz solution for modeling of piezoelectric energy harvester beams was due to Sodano *et al* [23], in which they considered a cantilevered bimorph without a tip mass with the following mechanical equation of motion:

$$\left(\underset{\sim}{M}_{\mathrm{s}}+\underset{\sim}{M}_{\mathrm{p}}\right)\ddot{\underset{\sim}{r}}(t)+\underset{\sim}{C}\dot{\underset{\sim}{r}}(t)+\left(\underset{\sim}{K}_{\mathrm{s}}+\underset{\sim}{K}_{\mathrm{p}}\right)\underset{\sim}{r}(t)$$
$$-\underset{\sim}{\Theta}\underset{\sim}{C}_{\mathrm{p}}^{-1}\underset{\sim}{q}(t)=\sum_{i=1}^{nf}\underset{\sim}{\phi}^{\mathrm{T}}(x_i)f_i(t). \tag{21}$$

Here, they [23] directly used the mechanical forcing function given by Hagood *et al* [21] on the right-hand side (the under tilde represents a matrix or a vector; see [23] for the remaining terms). In the original work, Hagood *et al* [21] defined discrete forces acting on *nf* coordinates $(x_1, x_2, \ldots, x_{nf})$ of the system. However, the base excitation problem does not include such a set of discrete forces. After concluding that the problem needed a new set of mode shapes due to the moving clamped boundary, Sodano *et al* [23] found it convenient to represent the mechanical forcing function as

$$f(t)=\int\int_V\int \rho A\omega^2\sin(\omega t)\,\mathrm{d}V \tag{22}$$

which, apparently, is nothing but the *total* beam mass times the base acceleration as the acceleration term $A\omega^2\sin(\omega t)$ can be taken outside the integrand. The same formulation was very recently used by Liu and Sodano [25] for a similar base excitation problem.

A correct implementation of Hagood *et al*'s discrete forces to base excitation was due to duToit *et al* [10], in which they concluded that the beam under base excitation has infinitely many discrete forces due to the local inertias of the infinitesimal elements, yielding an integral for the mechanical forcing term instead of the summation term in equation (21):

$$\underset{\sim}{M}\ddot{\underset{\sim}{r}}(t)+\underset{\sim}{C}\dot{\underset{\sim}{r}}(t)+\underset{\sim}{K}\underset{\sim}{r}(t)-\underset{\sim}{\Theta}\,\underset{\sim}{v}(t)=-\ddot{w}_{\mathrm{B}}\int_0^L m\underset{\sim}{\phi}^{\mathrm{T}}(x)\,\mathrm{d}x \tag{23}$$

where m is the mass per unit length of the beam, $\ddot{w}_{\mathrm{B}}$ is the base acceleration, and the remaining terms can be found in [10]. They [10] also presented an expression for the right-hand-side forcing function in equation (23) in the presence of a proof mass.

For the general case of the base excitation problem for a cantilevered beam with a proof mass located at the tip (as in figure 2), Elvin and Elvin [24] presented the following compact form:

$$\underset{\sim}{M}\ddot{\underset{\sim}{r}}(t)+\underset{\sim}{C}\dot{\underset{\sim}{r}}(t)+\underset{\sim}{K}\underset{\sim}{r}(t)-\underset{\sim}{\Theta}\,\underset{\sim}{v}(t)$$
$$=-\ddot{w}_{\mathrm{B}}\left(\int_0^L m\underset{\sim}{\phi}(x)\,\mathrm{d}x+M_{\mathrm{t}}\underset{\sim}{\phi}(L)\right) \tag{24}$$

where $\underset{\sim}{\phi}(x)$ is the vector of admissible functions, and the remaining terms can be found in [24]. Note that the electrical term in equation (21) is given in terms of the electric charge $\underset{\sim}{q}(t)$, whereas it is given by the voltage term in equations (23) and (24).

It is very useful to observe the analogy between the mechanical forcing functions of the analytical model and the discrete (Rayleigh–Ritz) model from equations (20) and (24), respectively. Representation of base excitation as a forcing function becomes more involved for structures more complicated than a conventional cantilevered beam [26]. Handling of base excitation problems of continuous structures (beams and frames) is extensively discussed in texts on earthquake engineering (see, for instance, Chopra [27]).

3.4. *Use of the static sensing and actuation equations*

In the 1990s, several researchers were interested in developing analytical relations to predict the *static* behavior of piezoelectric sensors and actuators [28–30]. Among others, Smits and Choi [28] and Wang and Cross [29] derived constituent relations under different static loading conditions of cantilevered bimorphs (tip force, tip moment, and uniformly distributed pressure). Later, DeVoe and Pisano [30] used Timoshenko's approach [31] of modeling bi-metal thermostats for modeling the *static* behavior of piezoelectric multi-morph cantilever actuators.

Recently, Ajitsaria *et al* [19] attempted to combine the relations given the literature of *static* sensing and actuation with the *dynamic* problem of energy harvesting. Although they [19] gave the modal expansion (equation (16) here) as the general solution to the Euler–Bernoulli beam equation, Ajitsaria *et al* [19] tried to combine the dynamic Euler–Bernoulli beam equation with the *constant radius of curvature* relations presented by DeVoe and Pisano [30]. The assumption of constant radius of curvature is reasonable for cantilevers bent by a static tip force, but this assumption clearly fails in the dynamic problem where the radius of curvature changes over the beam length as well as with the excitation frequency. After attempting to represent the base excitation as a tip force (see section 3.3), they [19] used the voltage to static tip force equation given by Wang and Cross [29] (and others later) to estimate the voltage in open conditions without a resistive load. Clearly, using the *static* sensing and actuation relations (which were derived for a static tip force) yields highly inaccurate results in the *dynamic* vibration-based energy harvesting problem (which is usually associated with base excitation).

3.5. *Use of the static deflection pattern instead of the fundamental mode shape*

Another simplification encountered in the literature is due to using the static deflection pattern obtained by a static tip force

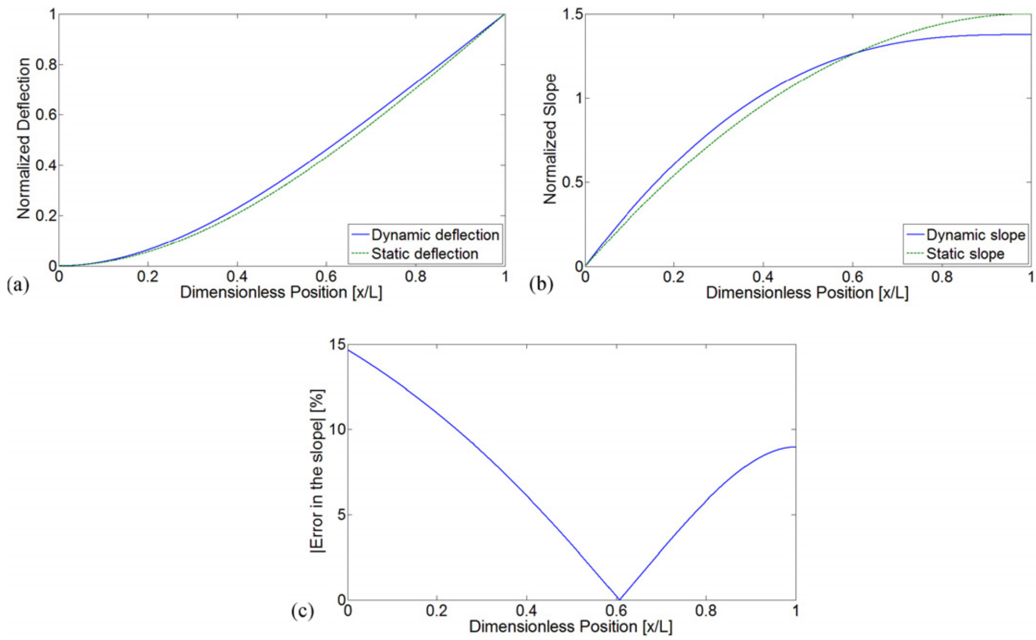

Figure 8. Comparison of the static and dynamic (a) deflection shapes, (b) slope distributions, and the (c) absolute value of the error in the slope due to using the static deflection expression.

with the assumption that it looks like the deflection pattern of the first vibration mode shape for clamped–free boundary conditions. Cornwell *et al* [32] studied energy harvesting from a cantilevered auxiliary structure attached to a three-story frame structure. The auxiliary structure (a cantilevered beam with a piezoceramic patch attached to the root) was excited from its base due to the motion of the three-story frame. After observing that the voltage response of the cantilever depends on the slope difference at the boundaries of the piezoceramic patch, Cornwell *et al* [32] used the following static deflection relation that gives the slope at point x on the beam in terms of the static deflection at the free end:

$$\frac{\mathrm{d}y_{\mathrm{st}}(x)}{\mathrm{d}x} = \frac{3y_a}{2L}\left[\frac{2x}{L} - \left(\frac{x}{L}\right)^2\right] \tag{25}$$

where y_a is the deflection at the free end (i.e., $y_{\mathrm{st}}(L) = y_a$) and L is the length of the beam. Equation (25) is derived for a cantilevered beam with a static tip force acting in the transverse direction, where the tip force term is eliminated by using the transverse stiffness ($3EI/L^3$) and the deflection y_a at the free end. The interpretation of Cornwell *et al* [32] regarding the relevance of the voltage output and the slope difference at the boundaries of the piezoceramic patch is correct (see equation (35) in [8] and equation (3) in [32]). However, they [32] considered a deflection pattern due to a static tip force assuming that the slope would not change significantly if one used the first mode shape instead. It is important to note that one of the natural boundary conditions to be satisfied at the free end of a clamped–free beam is *no transverse force* condition. The static deflection relations given for the case with a tip force directly violates this boundary condition as there is no tip force in the base excitation problem.

In the dynamic problem, for the same tip deflection amplitude (i.e., when $y_{\mathrm{dyn}}(L) = y_a$ is satisfied) the slope of the first vibration mode shape at point x can be given by

$$\frac{\mathrm{d}y_{\mathrm{dyn}}(x)}{\mathrm{d}x} = \frac{\lambda_1 y_a}{2L}\left[\left(\sinh\frac{\lambda_1 x}{L} + \sin\frac{\lambda_1 x}{L}\right) - \sigma_1\left(\cosh\frac{\lambda_1 x}{L} - \cos\frac{\lambda_1 x}{L}\right)\right] \tag{26}$$

where $\lambda_1 = 1.875\,104\,07$ is the eigenvalue of the first mode and $\sigma_1 = 0.734\,095\,514$ is a modal parameter (for a uniform cantilever without a tip mass). Note that equations (25) and (26) are such that the tip deflections at the free end are the same, i.e., $y_{\mathrm{st}}(L) = y_{\mathrm{dyn}}(L) = y_a$. This is displayed in figure 8(a), in which $y_{\mathrm{st}}(x)$ and $y_{\mathrm{dyn}}(x)$ are plotted together. For the static and dynamic deflection curves given in figure 8(a), the slope distributions are plotted in figure 8(b.) Note that equations (25) and (26) are made dimensionless since y_a/L is the same in both cases. Figure 8(b) shows that, for the same tip deflection amplitude, the slope distribution obtained from equation (25) is different from that obtained from equation (26). Reasonably, assuming the dynamic solution to be the accurate one, one can plot the absolute value of the error in the slope over the beam length due to using the static relation (figure 8(c)). Depending on the location of the piezoceramic patch on the beam, the error in the voltage prediction may be significant. Although it is not the case in Cornwell *et al* [32], for a piezoceramic patch having 20% of the total beam length located at the root (which is a very preferable location due to the large mechanical strain at the root), the voltage prediction with static deflection pattern may yield an error larger than 10% in the voltage amplitude, and an error larger than 20% in the power amplitude for a given load resistance.

Note that the discussion in this section is given for a uniform cantilevered beam without a tip mass. It is worth adding that, if one still prefers using a polynomial

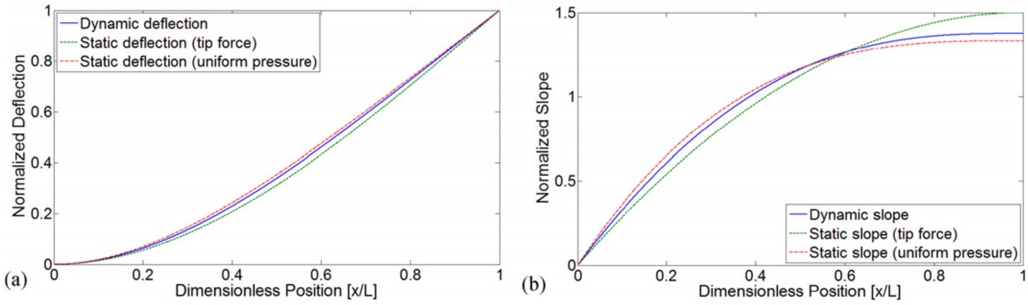

Figure 9. Comparison of the static and dynamic (a) deflection shapes and (b) slope distributions, showing the improvement in the static solution due to considering a uniform pressure loading.

representation based on the static deflection relation, the deflection formula for a uniform pressure loading [33] (rather than a concentrated tip force) should be preferred in the base excitation problem when there is no tip mass. As mentioned in section 3.3, the base excitation of a uniform beam without a tip mass is similar to the uniform pressure excitation of the respective stationary beam[6]. Figure 9(a) shows the deflection comparison for the first mode shape (dynamic deflection) of a uniform cantilever without a tip mass, static deflection due to a tip force, and static deflection due to uniform pressure. The same normalization used in figure 8 is applied in figure 9. The slope distribution over the beam length is given in figure 9(b). Note that the static deflection due to uniform pressure loading predicts the first mode shape and the slope distribution of a cantilevered beam without a tip mass better than the static deflection due to a tip force.

3.6. Closed-form analytical equations from the distributed parameter solution

After the analytical solution attempts based on Euler–Bernoulli beam theory and the approximate solutions with Rayleigh–Ritz discretization, recently, the closed-form expressions have been derived [8, 9] based on the Euler–Bernoulli assumptions, and attention was given to the issues discussed in the previous sections. That is, the piezoelectric coupling is treated accurately based on equation (4), modal expansion is assumed in the form of equation (16), and the base excitation is represented in the formal way as discussed with equations (19) and (20) here.

For a unimorph cantilever (figure 2(a)) excited by the motion of its base by harmonic translation $g(t) = Y_0 e^{j\omega t}$ and harmonic small rotation $h(t) = \theta_0 e^{j\omega t}$, the steady state voltage response across the resistive load is given by (from [8])

$$v_u(t) = \frac{\displaystyle\sum_{r=1}^{\infty} \frac{jm\omega^3 \varphi_r \left(\gamma_r^w Y_0 + \gamma_r^\theta \theta_0\right) e^{j\omega t}}{\omega_r^2 - \omega^2 + j2\zeta_r\omega_r\omega}}{\displaystyle\sum_{r=1}^{\infty} \frac{j\omega\chi_r\varphi_r}{\omega_r^2 - \omega^2 + j2\zeta_r\omega_r\omega} + \frac{1 + j\omega\tau_c}{\tau_c}} \tag{27}$$

[6] The problem becomes a combination of pressure excitation and tip force excitation when a tip mass is added to the beam. Reasonably, it converges to the tip force excitation problem if the tip mass is much larger than the distributed mass of the beam.

and the coupled steady state displacement response at point x on the harvester beam relative to its base is

$$w_{rel}(x,t) = \sum_{r=1}^{\infty} \left[\left(\gamma_r^w Y_0 + \gamma_r^\theta \theta_0\right) - \chi_r \left(\frac{\displaystyle\sum_{r=1}^{\infty} \frac{j\omega\varphi_r \left(\gamma_r^w Y_0 + \gamma_r^\theta \theta_0\right)}{\omega_r^2 - \omega^2 + j2\zeta_r\omega_r\omega}}{\displaystyle\sum_{r=1}^{\infty} \frac{j\omega\chi_r\varphi_r}{\omega_r^2 - \omega^2 + j2\zeta_r\omega_r\omega} + \frac{1 + j\omega\tau_c}{\tau_c}} \right) \right] \times \frac{m\omega^2 \phi_r(x) e^{j\omega t}}{\omega_r^2 - \omega^2 + j2\zeta_r\omega_r\omega} \tag{28}$$

where the relevant terms can be found in [8]. Note that both the voltage and the vibration response expressions given by equations (27) and (28) include the piezoelectric coupling information given by equation (4). Quite recently, Elvin and Elvin [24] have shown the convergence of the piezoelectrically coupled Rayleigh–Ritz solution (based on the formulations given by Hagood *et al* [21] and Crandall *et al* [22], as mentioned in section 3.3) to the closed-form analytical solution (equations (27) and (28) above) given by Erturk and Inman [8], if a sufficient number of admissible functions are used in the Rayleigh–Ritz discretization. In addition, it can be observed that the form of the fundamental mode Rayleigh–Ritz equations [15] is in agreement with the single-mode analytical equations (14) and (15).

The bimorph counterparts of equations (27) and (28) are presented in [9] along with experimental validations. Assuming that the base does not rotate ($\theta_0 = 0$), for excitation frequencies very close to the natural frequency of the rth vibration mode ($\omega \cong \omega_r$), the *multi-mode* equations (27) and (28) reduce to the *single-mode* equations (12) and (13).

4. Summary and conclusions

Piezoelectric transduction has received much attention for vibration-based energy harvesting over the past five years. The community working on piezoelectric energy harvesting includes researchers from mechanical, electrical, materials and civil engineering areas, and this community has been growing very rapidly. Several papers have appeared on modeling and applications of piezoelectric energy harvesters. Basically, a cantilevered beam with one or two piezoceramic layers mounted on a vibrating host structure is investigated as a typical piezoelectric energy harvester. Different authors from various engineering disciplines have presented their work on electromechanical modeling of these piezoelectric energy harvesters in the literature. Certain issues have been observed in some of the existing models, and some modeling errors have been repeated and propagated by different research groups. Hence, the motivation of this paper is to address these modeling problems and provide the necessary corrections for the existing and the future members of this community requiring the use of mathematical models for piezoelectric energy harvesters.

Here the existing problems are investigated under two topics as issues in SDOF modeling and issues in distributed parameter modeling, and clarifications are provided, with improved models and examples. The problems in SDOF modeling concern modeling of piezoelectric coupling and deficiencies of the existing SDOF piezoelectric energy harvester relations. Single-mode relations obtained from a recently proposed distributed parameter solution are presented as an alternative to the existing SDOF relations.

Predicting the electromechanical behavior of piezoelectric energy harvesters accurately requires deriving a distributed parameter model. Therefore, several researchers have attempted to obtain a distributed parameter solution based on Euler–Bernoulli beam theory and the fundamentals of piezoelectricity. In addition to the analytical solution attempts, approximate solution techniques in the sense of Rayleigh–Ritz discretization have appeared in the literature. The problems associated with the existing distributed parameter models include ignoring the effects of modal expansion and the resonance phenomenon, not modeling the piezoelectric coupling in the mechanical equation or its treatment as simple viscous damping, misrepresentation of the mechanical forcing term due to base excitation, and use of the static sensing and actuation equations and of the static deflection pattern in a dynamic problem. Some of these issues have resulted in fundamentally incorrect conclusions in the respective papers. For instance, the exclusion of resonance results in an incorrect electrical power frequency response, whereas leaving out the piezoelectric coupling in the beam equation fails to predict the resonance frequency variation with load resistance (as the system moves from short circuit to open circuit conditions) and yields inaccurate values for the optimum load resistance. These issues are addressed and clarified here for researchers interested in mathematical modeling of piezoelectric energy harvesters.

As is typical in the development of most new technologies, engineers rightfully start with primitive models to investigate new possibilities. As the disciplines mature, higher fidelity models are required in order to capture important subtleties and physical phenomena. Unfortunately, older more simplistic and even incorrect models are often propagated in the literature. The goal of this paper is to clarify the current state of modeling in piezoelectric-based energy harvesting.

Acknowledgments

The authors gratefully acknowledge the support of the Air Force Office of Scientific Research MURI under grant number F 9550-06-1-0326 ‘Energy Harvesting and Storage Systems for Future Air Force Vehicles’, monitored by Dr B L Lee.

References

[1] Anton S R and Sodano H A 2007 A review of power harvesting using piezoelectric materials 2003–2006 *Smart Mater. Struct.* **16** R1–21

[2] Williams C B and Yates R B 1996 Analysis of a micro-electric generator for microsystems *Sensors Actuators* A **52** 8–11

[3] Stephen N G 2006 On energy harvesting from ambient vibration *J. Sound Vib.* **293** 409–25

[4] *IEEE Standard on Piezoelectricity* 1987 (New York: IEEE)

[5] Jeon Y B, Sood R, Jeong J H and Kim S 2005 MEMS power generator with transverse mode thin film PZT *Sensors Actuators* A **122** 16–22

[6] Fang H-B, Liu J-Q, Xu Z-Y, Dong L, Chen D, Cai B-C and Liu Y 2006 A MEMS-based piezoelectric power generator for low frequency vibration energy harvesting *Chin. Phys. Lett.* **23** 732–4

[7] Priya S 2007 Advances in energy harvesting using low profile piezoelectric transducers *J. Electroceram.* **19** 167–84

[8] Erturk A and Inman D J 2008 A distributed parameter electromechanical model for cantilevered piezoelectric energy harvesters *ASME J. Vib. Acoust.* **130** 041002

[9] Erturk A and Inman D J 2008 An experimentally validated bimorph cantilever model for piezoelectric energy harvesting from base excitations *Smart Mater. Struct.* in review

[10] duToit N E, Wardle B L and Kim S-G 2005 Design considerations for MEMS-scale piezoelectric mechanical vibration energy harvesters *Integr. Ferroelectr.* **71** 121–60

[11] Erturk A and Inman D J 2008 On mechanical modeling of cantilevered piezoelectric vibration energy harvesters *J. Intell. Mater. Syst. Struct.* **19** at press (doi:10.1177/1045389X07085639)

[12] Roundy S, Wright P and Rabaey J 2003 A study of low level vibrations as a power source for wireless sensor nodes *Comput. Commun.* **26** 1131–44

[13] Roundy S, Wright P and Rabaey J 2004 *Energy Scavenging for Wireless Sensor Networks with Special Focus on Vibrations* (Boston, MA: Kluwer–Academic)

[14] Strutt J W (Lord Rayleigh) 1894 *The Theory of Sound* (London: MacMillan)

[15] duToit N E and Wardle B L 2007 Experimental verification of models for microfabricated piezoelectric vibration energy harvesters *AIAA J.* **45** 1126–37

[16] Lu F, Lee H and Lim S 2004 Modeling and analysis of micro piezoelectric power generators for micro-electromechanical-systems applications *Smart Mater. Struct.* **13** 57–63

[17] Chen S-N, Wang G-J and Chien M-C 2006 Analytical modeling of piezoelectric vibration-induced micro power generator *Mechatronics* **16** 397–387

[18] Lin J H, Wu X M, Ren T L and Liu L T 2007 Modeling and simulation of piezoelectric MEMS energy harvesting device *Integr. Ferroelectr.* **95** 128–41

[19] Ajitsaria J, Choe S Y, Shen D and Kim D J 2007 Modeling and analysis of a bimorph piezoelectric cantilever beam for voltage generation *Smart Mater. Struct.* **16** 447–54

[20] Beeby S P, Tudor M J and White N M 2006 Energy harvesting vibration sources for microsystems applications *Meas. Sci. Technol.* **13** 175–95

[21] Hagood N W, Chung W H and Von Flotow A 1990 Modelling of piezoelectric actuator dynamics for active structural control *J. Intell. Mater. Syst. Struct.* **1** 327–54

[22] Crandall S H, Karnopp D C, Kurtz E F Jr and Pridmore-Brown D C 1968 *Dynamics of Mechanical and Electromechanical Systems* (New York: McGraw-Hill)
[23] Sodano H A, Park G and Inman D J 2004 Estimation of electric charge output for piezoelectric energy harvesting *Strain* **40** 49–58
[24] Elvin N and Elvin A 2008 A general equivalent circuit model for piezoelectric generators *J. Intell. Mater. Syst. Struct.* at press (doi:10.1177/1045389X08089957)
[25] Liu Y and Sodano H A 2008 An investigation into active piezoelectric nanocomposites for distributed energy harvesting *Active and Passive Smart Structures and Integrated Systems*; *Proc. SPIE* **6928** 69280E
[26] Erturk A, Renno J R and Inman D J 2008 Modeling of piezoelectric energy harvesting from an L-shaped beam-mass structure with an application to UAVs *J. Intell. Mater. Syst. Struct.* at press (doi:10.1177/1045389X08098096)
[27] Chopra A K 2007 *Dynamics of Structures: Theory and Applications to Earthquake Engineering* (Englewood Cliffs, NJ: Prentice-Hall)
[28] Smits J G and Choi W S 1991 The constituent equations of piezoelectric heterogeneous bimorphs *IEEE Trans. Ultrason. Ferroelectr. Freq. Control* **38** 256–70
[29] Wang Q M and Cross L E 1999 Constitutive equations of symmetrical triple layer piezoelectric benders *IEEE Trans. Ultrason. Ferroelectr. Freq. Control* **46** 1343–51
[30] DeVoe D L and Pisano A P 1997 Modeling and optimal design of piezoelectric cantilever microactuators *J. Microelectromech. Syst.* **6** 266–70
[31] Timoshenko S 1925 Analysis of bi-metal thermostats *J. Opt. Soc. Am.* **11** 233–56
[32] Cornwell P J, Goethal J, Kowko J and Damianakis M 2005 Enhancing power harvesting using a tuned auxiliary structure *J. Intell. Mater. Syst. Struct.* **16** 825–34
[33] Pilkey W D 2005 *Formulas for Stress, Strain, and Structural Matrices* (New Jersey: Wiley)